European Journal of Medicinal Chemistry 95 (2015) 464–472

Contents lists available at ScienceDirect

European Journal of Medicinal Chemistry

journal homepage: http://www.elsevier.com/locate/ejmech

Original article

Synthesis, characterization and anticancer activity of gold(I) complexes that contain tri-*tert*-butylphosphine and dialkyl dithiocarbamate ligands

Muhammad Altaf [b], M. Monim-ul-Mehboob [a], Adam A.A. Seliman [a], Manzar Sohail [b], Mohammed I.M. Wazeer [a], Anvarhusein A. Isab [a, *], L. Li [c], V. Dhuna [d], G. Bhatia [d], K. Dhuna [d]

[a] *Department of Chemistry, King Fahd University of Petroleum and Minerals, Dhahran 31261, Saudi Arabia*
[b] *Center of Excellence in Nanotechnology, King Fahd University of Petroleum and Minerals, Dhahran 31261, Saudi Arabia*
[c] *King Abdullah University of Science and Technology (KAUST), Thuwal, 23955-6900 Jeddah, Saudi Arabia*
[d] *Deptartment of Molecular Biology and Biochemistry, Guru Nanak Dev University, Amritsar 143005, Punjab, India*

A R T I C L E I N F O

Article history:
Received 11 November 2014
Received in revised form
8 March 2015
Accepted 9 March 2015
Available online 10 March 2015

Keywords:
Gold(I) complexes
Anticancer activity
Human A549
MCF7 and HeLa cell lines

A B S T R A C T

Two new gold(I) complexes that contain tri-ter-butylphosphine and dialkyl dithiocarbamate ligands were synthesized and characterized by FTIR, NMR spectroscopy, Cyclic voltammetry, elemental analysis and X-ray diffraction. The *in vitro* cytotoxicity of both complexes was examined against A549 (lung cancer), MCF7 (breast cancer), and HeLa (cervical cancer) human cancer cell lines. Both complexes exhibit very strong *in vitro* cytotoxic effects against A549, MCF7 and HeLa cell lines. The screening of the cytotoxic activity based on IC_{50} data against the A549, MCF7, and HeLa lines shows that the synthesized gold(I) complexes are highly effective, particularly against HeLa cancer cell line. Based on IC_{50} data, the cytotoxic activity of both complexes is better than well-known commercial anticancer drug cisplatin against all the three cancer lines tested.

1. Introduction

Cisplatin, carboplatin and oxaliplatin are widely used commercial platinum(II) based metallo-drugs which have been used effectively for the treatment of cancers [1–3]. However, the gamut of activity against different kinds of cancers is limited for such drugs [4]. The efficacy of platinum(II) anticancer drugs is mainly hampered due to some side effects such as neurotoxicity, ototoxicity, anemia, nausea [5] and the acquired as well as intrinsic resistances exhibited by cancer cell lines [6]. Such negative and limiting factors of platinum(II) drugs are major impediments in their clinical use invariably against all kind of cancers [7]. Therefore, non-platinum metals like gold compounds have been synthesized and evaluated for their potential augmented anticancer activity with much lower toxicity and fewer side effects against a wide panel of cancer cell lines.

Generally, the study of gold complexes, bearing different functional ligands exhibiting interesting physical, chemical, biological and pharmacological properties, has gained much attention [8–11]. Particularly, there was substantial interest in the coordination chemistry of Au(I) complexes showing biological activity with potential medicinal applications. For instance, the currently used drugs like *Auranofin*, *Solganol* and *Myocrisin* are Au(I)–S complexes [12–16]. Consequently, the gold(I) complexes have long been studied as anti-arthritic and anti-microbial agents [17–21]. It has been found that gold(I)-phosphine complexes with P–Au–P, P–Au–N, P–Au–S, and S–Au–S bonding show marked biological activities against bacteria and yeast [22,23]. The gold(I) phosphine complexes are known to exhibit promising anticancer properties [17,24–26].

In this connection, Lorber *et al.* firstly reported in 1979 that *Auranofin* could inhibit the *in vitro* proliferation of HeLa cells [27]. McKeage and coworkers reported, bis(diphosphino)gold(I) compounds demonstrate prospective *in vivo* anticancer activities [28]. Berners-Price *et al.* pointed out $[Au(dppe)_2]^+$ and its derivatives as their credible *in vitro* and *in vivo* anticancer activities *via* the

* Corresponding author.
E-mail address: aisab@kfupm.edu.sa (A.A. Isab).

http://dx.doi.org/10.1016/j.ejmech.2015.03.019

mitochondrial-mediated apoptotic pathway [29]. V. Gandin et al. reported that phosphine gold(I) complexes efficiently inhibited cytosolic and mitochondrial (TrxR) [30]. Ott *et al.* reported gold(I) phosphine complex containing naphthalimide ligand behaves as a TrxR inhibiting antiproliferative agent and angiogenesis inhibitor [31]. Che *et al.* described anticancer gold(I)-phosphine complexes as potent autophagy-inducing agents [32].

In the last decade, a new class of gold complexes with dithiocarbamate ligands has been emerged as potential anticancer agents. In this regards, Fregona and coworkers firstly prepared and characterized some novel gold(III) dithiocarbamate compounds containing N,N-dimethyldithiocarbamate and ethylsarcosinedithiocarbamate exhibiting the promising chemical and biological profile [33]. Similarly, significant inhibitory effect of dibromo(N,N- dimethyldithiocarbamato)gold(III) *in vivo* was reported against growth of MDA-MB-231 breast tumor cells (BTC) [34]. Gold(I)-dithiocarbamato species, could inhibit the chymotrypsin-like activity of purified 20S proteasome and 26S proteasome in human breast cancer MDA-MB-231 cells [35].

Gold(I) thiolates employed clinically in the treatment of rheumatoid arthritis displayed some potency against various tumors but a greater potential is found in their analogs. In particular, analogs featuring a linear P–Au–S arrangement in which the thiolate ligand is derived from a biologically active thiol display high potency [36]. Recently, Keter *et al.* synthesized new gold(I) complexes containing PPh_3 = triphenyphosphine or dppp = 1,3-bis(diphenylphosphino)propane or dpph = 1,6-bis-(diphenylphosphino)hexane and L = pyrazolyldithiocarbamate or 3,5-dimethylpyrazolyldithiocarbamate or indazolyldithiocarbamate and found all complexes active against human cervical epithelioidcarcinoma (HeLa) cells [37]. Here, we are reporting the synthesis of gold(I) complexes of tertiarybutylphosphine with dialkyl dithiocarbamate as co-ligands, their structure determination by single crystal X-ray crystallography and their structural analysis by FTIR and NMR measurements. Finally, the well characterized gold(I) complexes have been subjected to *in vitro* cytotoxic evaluation against three standard human cancer cell lines named, A549, MCF7, and HeLa cell lines.

2. Materials and physical methods

Sodium dimethyldithiocarbamate monohydrate, sodium diethyldithiocarbamate trihydarte were purchased from Sigma–Aldrich Co. St. Louis, Missouri United States. Chloro(tri-tert-butylphosphine)gold(I) (**1**) as gold(I) precursor was obtained from Strem Chemicals, Inc., Newburyport, Massachusetts, United States. All solvents including ethanol and dichloromethane were purchased from Merck Darmstadt, Germany and used without further purification. All reactions were carried out under normal ambient conditions. Human lung cancer, human breast cancer and human cervical cancer cell lines were procured from National Centre for Cell Sciences (NCCS), Pune, India.

Elemental analyses of (dialkyldithiocarbamato) (tert-butylphosphine)gold(I) complexes (**2** and **3**) were performed on Perkin Elmer Series 11 (CHNS/O), Analyzer 2400. The solid state FTIR spectra of free ligands and their corresponding gold(I) complexes were recorded on a Perkin–Elmer FTIR 180 spectrophotometer or NICOLET 6700 FTIR using Potassium bromide (KBr) pellets over the range 4000–400 cm^{-1} and Far-IR spectra were recorded for gold complexes at 4 cm^{-1} resolution at room temperature using Cesium chloride (CsCl) disks on a Nicolet 6700 FTIR with Far-IR beam splitter. The IR frequencies (cm^{-1}) of free ligands and Au(I) complexes are given in Table 1.

^{1}H, ^{13}C, and ^{31}P NMR spectra were recorded on a LAMBDA 500 spectrophotometer operating at 500.01, 125.65 and 200.0 MHz respectively, corresponding to a magnetic field of 11.74 T. Tetramethylsilane (TMS) was used as an internal standard for ^{1}H and ^{13}C, while Triphenylphosphine (TPP) was used as an external standard for ^{31}P NMR spectra. The ^{13}C NMR spectra were obtained with ^{1}H broadband decoupling, and the spectral conditions were: 32 k data points, 0.967 s acquisition time, 1.00 s pulse delay and 45 pulse angle. The ^{1}H, ^{13}C and ^{31}P NMR chemical shifts are given in Tables 2 and 3, respectively. Skeletal structures and condensed formulae of the complexes (**1**–**3**) representing non-equivalent carbons and protons are shown in Scheme 1.

3. Results and discussion

3.1. FTIR characterization

Dithiocarbamate compounds can be identified *via* the presence of certain absorbance peaks primarily vibrational ν(C–N) and ν(C–S). In the infrared spectra of dithiocarbamate compounds, the region 1480–1550 cm^{-1} is primarily associated with the $R_2N–CS_2$ 'thioureide' band which defines the carbon–nitrogen bond order between a single bond at 1250–1350 cm^{-1} and a double bond at 1640–1690 cm^{-1} [38].

In the IR spectra, the most important thioureide band, *ν*(C–N) was observed at 1479 and 1478 cm^{-1} for complexes **(2)** and **(3)** respectively. Since these frequency modes lie in between those associated with single C–N and double C=N bonds hence the partial double bond character of thioureide bond was confirmed for both of the complexes [39]. The presence of thioureide band between 1430 and 1545 cm^{-1} suggests a considerable double bond character in the C–N bond vibration of the $R_2N–CS_2$ group [40]. This strong absorption band (1480–1542 cm^{-1}) is known as the thioureide ion band. The band appears intermediate within C–N single bond (C–N: 1063–1261 cm^{-1}) and double bond (C=N: 1640–1690 cm^{-1}). This band shows the partial double bond characteristic of dithiocarbamate (S_2C-NR_2). Such partial double bond culminates into stretching vibration due to the partial delocalization of electron density within the dithiocarbamate moiety [41]. A strong absorption band in the range of 1480–1542 cm^{-1} gives additional confirmation of the gold(I) complexes formation [42].

The C=S thiocarbonyl stretch splits into two peaks (doublet) at 1022, 972 cm^{-1} and 1020, 989 cm^{-1} with medium intensity in the spectra of complexes **(2)** and **(3)** respectively. The bands present in the range of 972–1022 cm^{-1} is attributed to the customary contribution of (C … S). The splitting of ν(C–S) bands in the range 965–972 cm^{-1} indicates a monodentate nature of dialkyl dithiocarbamate ligands in the synthesized complexes [43–45]. In addition to the polar thioureide ion band, the usual bands for sp^3-hybridized carbon–hydrogen stretches are observed in the range of 2840–3000 cm^{-1} [46]

The stretching band frequencies are observed for the saturated aliphatic C–H methyl group of coordinated dialkyl (methyl/ethyl) dithiocarbamate at 2962(asym), 2869(sym) and 2965(asym), 2867(sym) cm^{-1} for complexes **(2)** and **(3)** respectively. The C–H ($-CH_3$) methyl groups have characteristic bending absorptions at 1372 and 1371 cm^{-1} in the spectra of complexes **(2)** and **(3)** respectively. The C–H bending band(s) associated C–H stretching band(s) are often determining factor of methyl groups in a molecule. The C–H ($-CH_2-$) methylene coordinated diethyldithiocarbamate stretching occurs at 2925 cm^{-1} and its corresponding bending appears at 1409 cm^{-1} for complex **(3)** [47,48].

The band at 304 cm^{-1} in the far-IR spectrum of complex (**1**) has been assigned to the *ν*(Au–Cl) vibration, while bands appearing at 282 and 194 cm^{-1} are attributed to *ν*(Au–S) and *ν*(Au–P) vibrations for complexes **(2)** and **(3)** respectively [49–53].

Table 1
IR frequencies (cm^{-1}) of free ligands and complexes (**2**) and (**3**).

Free ligand/complex	Stretch	Bend	Stretch	Bend	Stretch	Stretch
	C–H(CH_3)	C–H(CH_3)	C–H(CH_2)	C–H(CH_2)	C=S	S=C–N
Free dimethyl dithiocarbamate	2924	1360	–	–	962	1488
(**2**)	962(asym), 2869 (sym)	1372	–	–	1022, 972	1479
Free diethyldithiocarbamate	2925	1358	2979	1379	986	1466
(**3**)	2965(asym), 2867 (sym)	1371	2925	1409	1020, 989	1478

Table 2
Solution ^{1}H NMR chemical shifts (ppm) of the free gold(I) metal precursor (**1**) and complexes (**2**) and (**3**).

Free ligand/complex	2-H	4-H	5-H
(**1**)	1.52	–	–
Free $NaS_2CN(CH_3)_2 \cdot H_2O$	–	3.55	–
(**2**)	1.55	3.48	–
Free $NaS_2CN(C_2H_5)_2 \cdot 3H_2O$	–	1.23	4.03
(**3**)	1.53	1.31	3.92

Table 3
Solution ^{13}C and ^{31}P NMR chemical shifts (ppm) of the free gold(I) metal precursor (**1**) and Au(I) complexes (**2**) and (**3**).

Free ligand/complex	C=S	C-1	C-2	C-4	C-5	^{31}P
		(J_{PC} in Hz)				
(**1**)	–	39.42(20.6)	32.23	–	–	200.02
Free $NaS_2CN(CH_3)_2 \cdot H_2O$	212.82	–	–	45.12	–	–
(**2**)	207.49	39.31(17.5)	32.21	45.16	–	207.49
Free $NaS_2CN(C_2H_5)_2 \cdot 3H_2O$	206.7	–	–	49.61	12.31	
(**3**)	205.92	39.39(17.5)	32.24	49.03	12.21	205.87

3.2. NMR characterization

The ^{1}H NMR chemical shifts of gold(I) complexes **(1–3)** and free dialkyl dithiocarbamate ligands are listed in Table 2. A small upfield shift for methyl protons of tri-ter-butyl group was observed for complex **(2)** compared to complex **(1)**. Whereas, a small downfield shift for methyl protons of tri-*ter*-butyl group have been observed for complex (**3**) as shown in Table 2. The small upfield shifts for proton(s) of the coordinated dimethyldithiocarbamate and diethyldithiocarbamate have been observed in gold(I) complexes **(2** and **3)** in comparison to free dialkyl dithiocarbamate ligands.

The ^{13}C and ^{31}P NMR chemical shifts of complexes **(2)** and **(3)** along with their corresponding gold(I) precursor (**1**) and free dialkyl dithiocarbamate ligands are tabulated in Table 3. In the ^{13}C NMR spectra four and five resonances are observed for complexes (**2**) and (**3**) respectively. Small shielding in the chemical shifts was observed for methyl carbons and quaternary carbon bonded to phosphorus in tri-*ter*-butylphosphine in the complexes **(2** and **3)** as compare to gold(I) precursor. There are also small upfield chemical shifts for **C**H_3, **C**H_2 and **C**=S carbons of coordinated dialkyl dithiocarbamate with respect to free dialkyl dithiocarbamate ligands. The ^{13}C chemical shifts of C=S carbon of free dimethylthiocarbamate and diethylthiocarbamate ligands are observed in the range 206–213 ppm. The upfield shifts are observed for coordinated dialkyldithiocarbamates in complexes **(2)** and **(3)**. The P–C coupling constant ($J_{p\text{-}c}$) showed a reduction of 3 Hz on complexation.

3.3. Crystal structure of complex (2)

The molecular structure of complex (**2**) is shown in Fig. 1. X–ray structure contains one molecule of complex [t-$Bu_3PAu(S_2CNMe_2)$] (**2**) in crystallographic asymmetric unit. The monodentate mode of coordination of the dithiocarbamate ligand is reflected in the difference of C–S bond lengths with the shortest of these being associated with the weakly bonded S2 atom as shown in Table 4. The gold(I) atom is coordinated with P and S atoms of tri-*ter*-butylphosphine and dimethyl dithiocarbamate ligands respectively. The Au1–S1 and Au1–P1 bond distances are 2.3247 (15) and 2.2743 (14) Å respectively. The P1–Au1–S1 bond angle is 176.44 (4)°, which shows Au(I) atom adopts distorted linear geometry. The Au–S bond length is longer than Au–P bond length. The deviation from the ideal linear geometry around gold can be attributed to the presence of a close intra-molecular Au1 … S2 contact of 3.127 Å. The Au–S and Au–P bond lengths are similar to those found in [$Et_3PAu(S_2CNEt_2)$] complex [54]. However, the S–Au–P bond angle is different from [$Et_3PAu(S_2CNEt_2)$] complex [54] and other [t-Bu_3PAu]$^+$ complexes [55–58].

3.4. Crystal structure of complex (3)

X-ray structure of complex (**3**) is shown in Fig. 2. There are two independent molecules of gold(I) complex in the asymmetric unit cell. In both molecules, gold(I) atom is coordinated with one P donor atom of tri-*ter*-butylphosphine ligand and S atom of diethyldithiocarbamate ligand. There are only minor conformational differences between x-ray structure of two molecules.

The Au1–S1 and Au2–S3 bond distances are 2.3293 (15) and 2.3139 (16) Å respectively. The Au1–P1 and Au–P2 bond distances are 2.2818 (15) and 2.2753 (16) Å. The Au–S bond distances are very much similar to [t-$Bu_3PAu(S_2CNMe_2)$] (**2**) and [$Et_3PAu(S_2CNEt_2)$] complexes [54]. The Au–P bond distances are different than [$Et_3PAu(S_2CNEt_2)$] complex [54] and similar to [t-$Bu_3PAu(S_2CNMe_2)$] (**2**) complex.

The geometry around Au1 and Au2 atoms is conventionally distorted linear and similar to [t-$Bu_3PAu(S_2CNMe_2)$] (**2**) and [$Et_3PAu(S_2CNEt_2)$] complexes [60]. In molecules 1 and 2, S1–Au1–P1 and S3–Au2–P2 bond angles are 172.74 (6) and 170.42 (6)° respectively. More distortion from ideal linear geometry is observed in each molecule of complex (**3**) than complex (**2**). It is interesting to correlate the magnitude of the intra-molecular Au–S interactions with the deviations from linearity of the P–Au–S bond. In complex (**3**), where the Au1 … S2 and Au2 … S4 interactions are longer, the deviation from the ideal linear angle of 180° is increased. The bond angle values around central Au(I) atom in molecule 1 and 2 confirm the presence of pseudo linear geometry in complex (**3**). The overall geometry of [t-$Bu_3PAu(S_2CNEt_2)$] (**3**) closely resembles to those Au(I) complexes that contain [t-Bu_3PAu]$^+$ unit [55–58].

3.5. Electrochemical study of gold(I) complexes (1–3)

Cyclic Voltammetry of complexes (**1**, **2** and **3**) is given in Fig. 3. Quasireversible redox couple corresponding to [Au(t-BuP)Cl=^{0}/[Au(t-BuP)Cl]$^{2+}$ appears at 1.19 V while for complexes (**2** and **3**) this redox couple appears at 1.24 V and 1.41 V, respectively. Higher potentials for redox couples of complexes (**2** and **3**) are indicative of

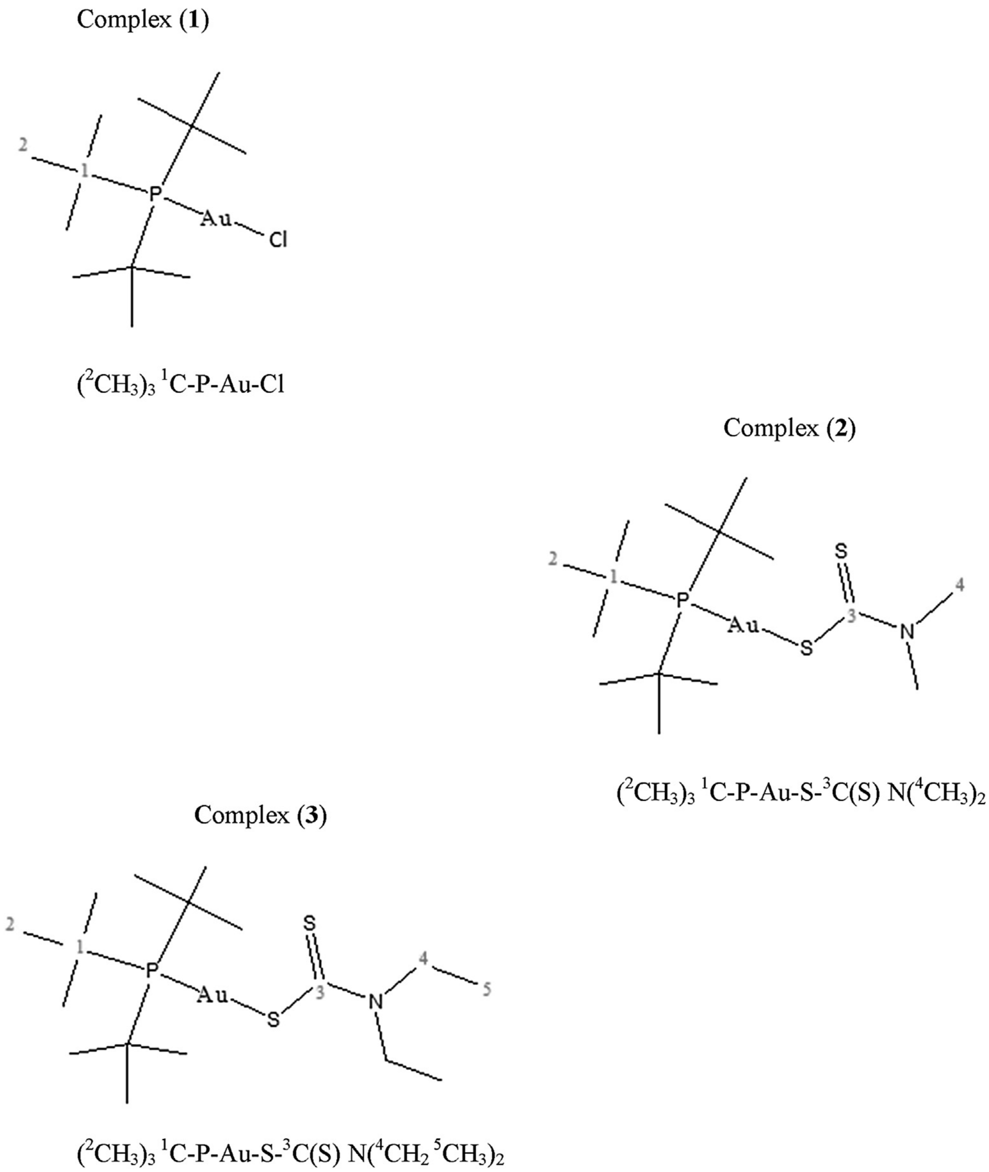

Scheme 1. Skeletal structures and condensed formulae of complexes (**1**), **(2)** and **(3)** representing non-equivalent carbons and protons for ^{13}C and ^{1}H NMR data.

the difficulty in gold(I) oxidation due to stabilizing effect of the dialkyl dithiocarbamate ligands [59]. Increase in chain length with corresponding increase in electron donating effect of alkyl groups of the ligands is responsible for a higher anoidic potential of complex (**3**) compared to complex (**2**). Thus, higher oxidation potentials of Au(I) in complexes (**2** and **3**) are indicative of their higher stability compared to complex (**1**) under physiological conditions. All three complexes show one reduction process, which is attributed to the gold(I) − gold(0) reduction. For complex (**1**) reduction peak appears at 0.167 V while for complex (**3**); it is at 0.0848 V and for complex (**2**) at −0.019 V.

3.6. *In vitro anticancer activities of complexes (**1–3**)*

Modern oncologic or anticancer studies aim towards finding newer compounds with less cytotoxic potential than cisplatin toxicity. In this connection, gold(I) complexes with various ligands including Au–N, Au–S or Au–C bonds are being extensively developed and investigated for their bioactivities as cytotoxic agents [60]. In this study, new gold(I) complexes (**2** and **3**) are developed by replacing one chlorido ligand in gold(I) precursor complex (**1**) with dialkyldithiocarbamto ligand. The synthesized complexes (**2** and **3**) are subjected *to in vitro* cytotoxic evaluation against A549, MCF7 and HeLa cancer cell lines using MMT assay.

The dose dependent cytotoxic effect was obtained by the stipulated increase in concentrations of complexes (**1**), (**2**) and (**3**) against the fixed number of human cancer cells as shown in Figs. 4–6. The IC_{50} concentration of complexes (**1**), (**2**) and (**3**) for different human cell lines are obtained from a curve between complex concentration and percentage viability of cells as shown in Figs. S1–S3. The IC_{50} values of all complexes are in the range of 2.11 ± 0.43 to 26.90 ± 1.04 μM as given in Table 4.

The *in vitro* cytotoxicity in terms of IC_{50} values against A549 cell line were found 41.60 ± 3.00, 14.30 ± 0.81, 26.90 ± 1.04 and 19.40 ± 0.64 μM for cisplatin and gold(I) complexes (**1**), (**2**) and (**3**) respectively. The precursor complex **(1)** and synthesized complexes **(2** and **3)** have shown cytotoxicity almost two-three folds better than cisplatin. In MCF7 cancer cell line, *in vitro* anticancer activity in

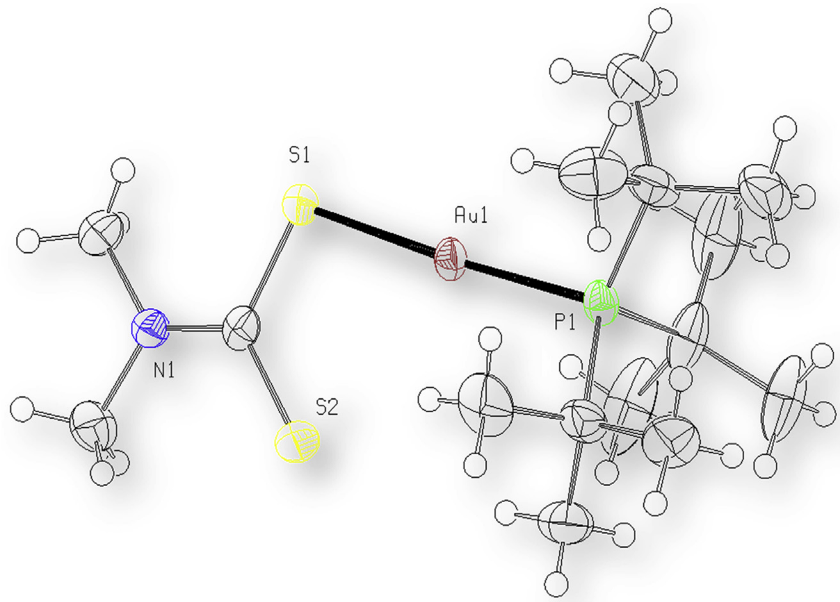

Fig. 1. A view of the molecular structure of mononuclear complex (**2**), with partial atom labeling scheme and displacement ellipsoids drawn at 50% probability level.

Table 4
IC_{50} Values (μM) of gold(I) complexes against A549, MCF7 and, HeLa cancer cell lines.

Complex	A549	MCF7	HeLa
Cisplatin	41.60 ± 3.00	22.38 ± 0.62	19.40 ± 1.85
(**1**)	14.30 ± 0.81	16.71 ± 0.80	16.03 ± 1.01
(**2**)	26.90 ± 1.04	21.07 ± 0.95	2.11 ± 0.43
(**3**)	19.40 ± 0.64	16.00 ± 0.83	3.18 ± 0.54

terms of IC_{50} values were 22.38 ± 0.62, 16.71 ± 0.80, 21.07 ± 0.95 and 16.00 ± 0.83 μM for cisplatin and gold(I) complexes (**1**), (**2**) and (**3**) respectively. The precursor complex **(1)** and synthesized complexes **(2 and 3)** have anticancer activity close to cisplatin. For HeLa cancer cell line, *in vitro* cytotoxicity in terms of IC_{50} values were 19.40 ± 1.85, 16.03 ± 1.01, 2.11 ± 0.43 and 3.18 ± 0.54 μM for cisplatin and gold(I) complexes (**1**), (**2**) and (**3**) respectively. Against HeLa cell line cytotoxicity of gold(I) complexes **(2 and 3)** is six to eight times better than cisplatin and gold(I) precursor complex (**1**). Newly synthesized complexes (**2**) and (**3**) were found to be most

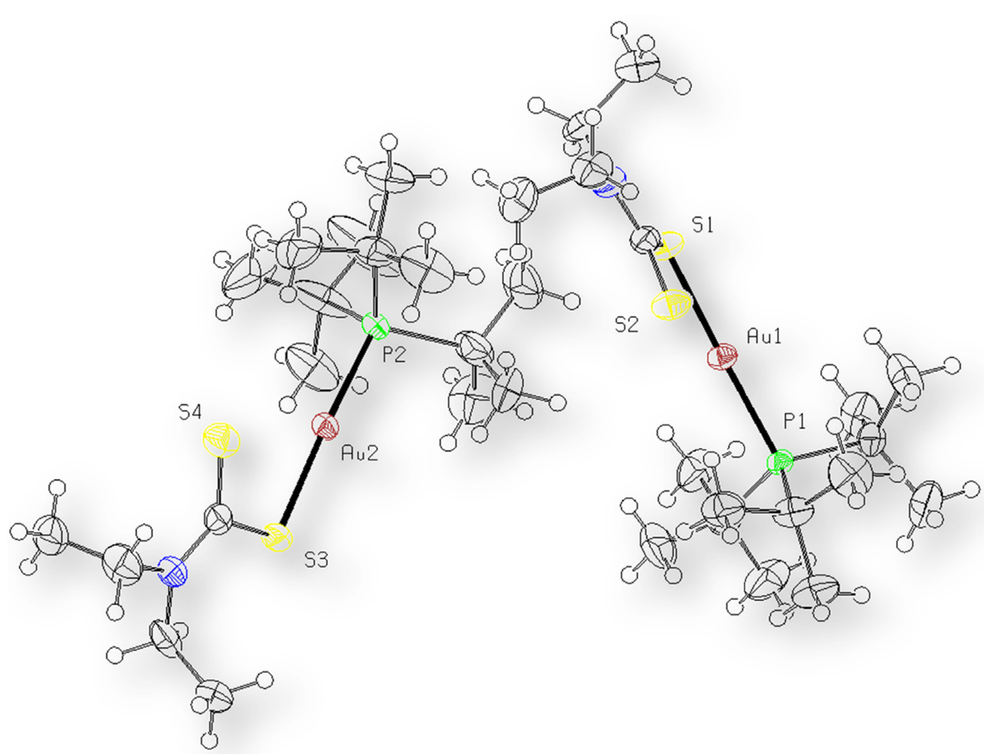

Fig. 2. A view of the molecular structure of mononuclear complex (**3**), with partial atom labeling scheme and displacement ellipsoids drawn at 50% probability level.

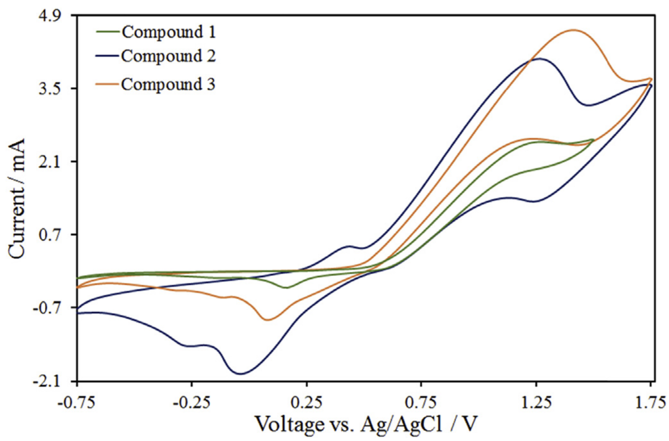

Fig. 3. Cyclic voltammograms of complexes (**1**, **2** and **3**) at platinum electrode.

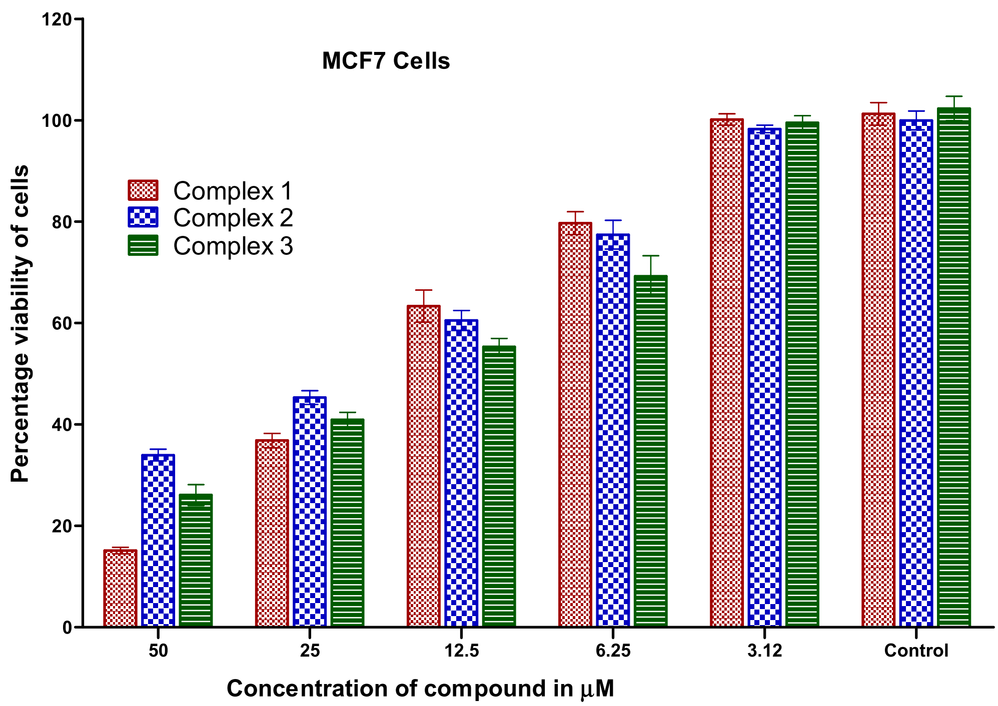

Fig. 4. Graph showing the cytotoxic effect of series of concentrations of compounds (**1**–**3**) on viability of MCF 7 cells.

effective against HeLa cell line in terms of IC_{50} values. Against HeLa cell line cytotoxicity of complexes (**2** and **3**) is better than the equivalent Au(PEt_3)Cl, "the following IC_{50} (μM) value against the same line show: Au(PEt3)Cl: 1.7(0.06) μM [61]".

The better inhibition of growth of cancer cells by synthesized complexes (**2** and **3**) than gold(I) precursor complex (**1**) can be attributed to dithiocarbamate as labile co-ligands bonded with central gold(I) ions. Overall, the anticancer activity of synthesized complexes (**2** and **3**) against, A549, MCF7 and HeLa human cancer cell lines is interesting and better activity than previous anticancer studies of gold compounds [62–65].

4. Conclusions

In this report, cytotoxic activity of two gold(I) complexes with S–Au–P fragment against A549, MCF7 and HeLa human cancer cell lines have been evaluated and these complexes exhibit very strong cytotoxic effects *in vitro*. The new complexes (**2** and **3**) with the dimethyldithiocarbamate and diethyldithiocarbamate ligands showed excellent cytotoxic activity against HeLa human cancer cell line. These results show good inhibition and selectivity of both complexes against HeLa cell line which is very important in drug design inhibition of target biomolecules. In short, the IC_{50} data reveals that complexes (**2** and **3**) are much better cytotoxic agents than commonly used cisplatin. The significant cytotoxicitic activity of gold(I) complexes (**2** and **3**) has made them strong candidates as potential anticancer agents for further exploration against cervical cancer.

5. Experimental

5.1. Synthesis of [t-Bu_3PAu(S_2CNMe_2)] (**2**)

Sodium dimethyldithiocarbamate monohydrate (0.072 g, 0.05 mmol) dissolved in 15 mL ethanol was added drop wise to [t-Bu_3PAuCl] (0.217 g, 0.05 mmol) contained in 10 mL dichloromethane at room temperature and solution was continuously stirred for 3h. The clear light yellow solution obtained was filtered to avoid any impurity and kept undisturbed at room temperature for crystallization by slow evaporation. After seven days colorless block like crystals were obtained. A suitable quality crystal was chosen for X-ray diffraction analysis. Anal. Calc. for $C_{15}H_{33}AuNPS_2$: C, 34.68; H, 6.40; N, 2.70; S, 12.34; Found: C, 34.80; H, 6.33; N, 2.82; S, 12.43. Yield: 0.242 g, (93%).

5.2. Synthesis of [t-Bu_3PAu(S_2CNEt_2)] (**3**)

Sodium diethyldithiocarbamate trihydrate (0.113 g, 0.05 mmol) dissolved in 15 mL of ethanol was added dropwise to [t-Bu_3PAuCl] (0.217 g, 0.05 mmol) contained in 10 mL dichloromethane at room temperature with continuous stirring for 3 h. The transparent yellow solution obtained was filtered to avoid any impurity and kept undisturbed for slow evaporation at room temperature. After five days

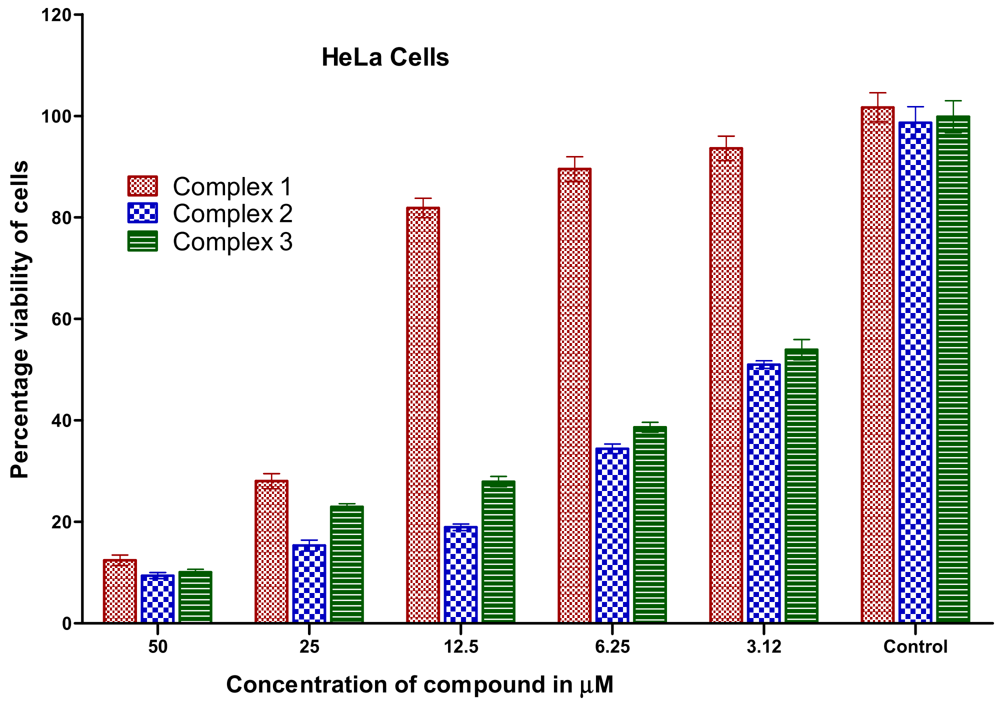

Fig. 5. Graph showing the cytotoxic effect of series of concentrations of compounds (**1**–**3**) on viability of HeLa cells.

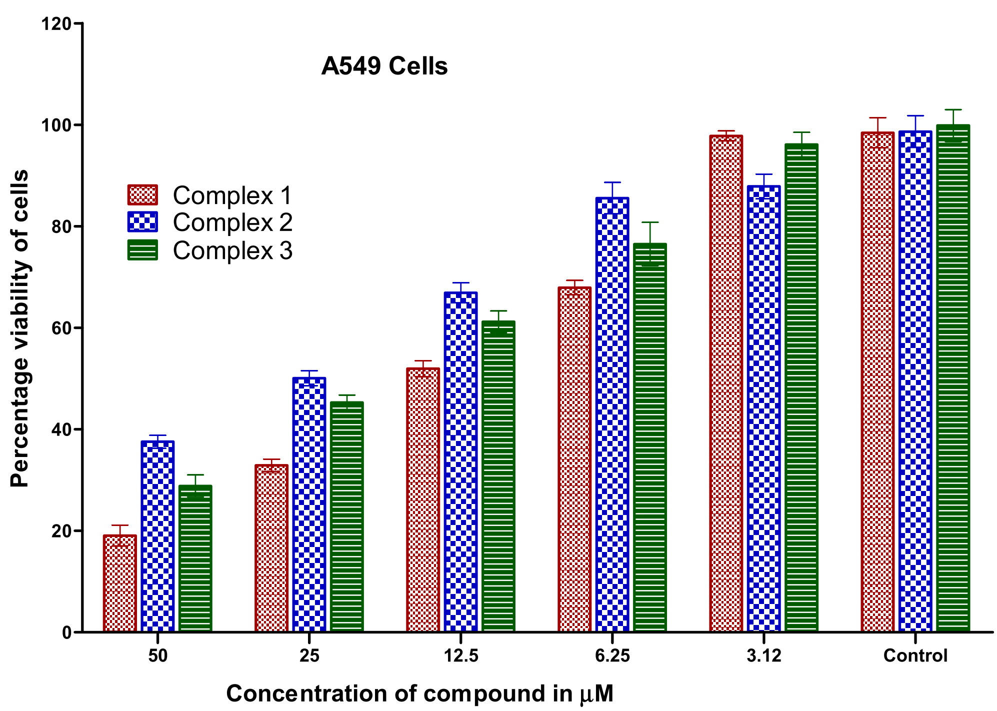

Fig. 6. Graph showing the cytotoxic effect of series of concentrations of compounds (**1**–**3**) on viability of A549 cells.

colorless block like crystals were obtained. A suitable quality crystal was chosen for X-ray diffraction analysis. Anal. Calc. for $C_{17}H_{37}AuNPS_2$: C, 37.29; H, 6.81; N, 2.56; S, 11.71; Found: C, 37.19; H, 6.37; N, 2.70; S, 11.68. Yield: 0.260 g, (95%).

5.3. Stability of gold(I) complexes in DMSO-d$_6$

^{1}H and NMR spectra of complexes (**2** and **3**) in DMSO-d$_6$ solvent were measured for their stability test. The extent of decomposition over time was determined by comparing the NMR spectra collected after 1, 6, 12, 24, 48 and 72 h. No significant change in the chemical shifts and the splitting patterns of complexes (**2** and **3**) were observed in their time dependent ^{1}H and ^{13}C NMR spectra.

5.4. X-ray structure determination

For both gold(I) complexes (**2**) and (**3**), good quality single crystal was chosen and mounted on a plastic loop to an Agilent

Super Nova diffractometer equipped with a Mo-Kα radiation (λ = 0.71073 Å). The data were collected and integrated with CrysAlisPRO [66]. The refinement and all further calculations were carried out using SHELXL [67]. The H–atoms were either located from Fourier difference maps and freely refined or included in calculated positions and treated as riding atoms using SHELXL default parameters. The non–H atoms were refined anisotropically, using weighted full–matrix least–squares on F^2. Empirical or multiscan absorption corrections were applied using the SCALE3 ABSPACK [68]. Graphics were generated using PLATON [69]. A summary of crystal data and refinement details for gold(I) complexes (**2**) and (**3**) are given in Table 5. Selected bond lengths and bond angles are given in Table 6.

5.5. Electrochemistry

Electrochemical measurements were undertaken on an Autolab PGSTAT-128N (Eco-Chemie) workstation. A standard three electrode electrochemical cell utilizing a membrane Pt-disc working electrode, a double junction Ag/AgCl/3M KCl reference electrode and platinum wire auxiliary electrode was used in all voltammetric experiments. 10 mM of all compounds were dissolved in acetonitrile containing 100 mM of Potassium thiocyanate as an electrolyte.

5.6. MTT assay for in vitro anticancer of complexes (**1**–**3**)

A549, MCF7 and HeLa human cancer cells were seeded and maintained on Dulbecco's Modified Eagle's Medium (DMEM) supplemented with streptomycin (100 U/mL), gentamycin (100 μg/mL), 10% FBS (Fetal Bovine Serum) at 37 °C and humid environment containing 5% CO_2. MTT was used to assess cell integrity and *in vitro* anticancer. The uptake of the vital mitochondrial dye, 3-[4,5-dimethylthiazol-2-yl]- 2,5-diphenyl tetrazolium bromide (MTT) was monitored by cell mitochondria [70]. The cells were grown in 96 well flat bottom tissue culture plates at a concentration of 5×10^3 cells/well in DMEM medium. After 72 h of growth, three cancer cell lines, A549, MCF7 and HeLa were treated with gold(1) complexes (**1**–**3**) and cisplatin at concentration from 3.12 to 50 μM. After 24 h, 100 μL of MTT was added to each well and incubated the plate for 4 h at 37 °C in dark. The treated plate was then removed and 100 μL of DMSO (Dimethylsulfoxide) was added in each well. Mixture in each well was subjected to mixing well by repeated pipetting in and out to bring out the formazan. The absorbance was read out at 570 nm in ELISA (Enzyme-linked immunosorbent assay) reader. The cell viability values were expressed as the mean ± standard error of the mean (SEM) from at least three independent experiments. The IC_{50} concentrations of gold(1) complexes (**1**–**3**) used were calculated from a separate curve between complex concentration and average % viability of cells plotted in Microsoft Excel 2007 (graphs not shown) using MTT assay data and explained by logarithmic regression equations (equations not shown).

Table 5
Crystallographic characteristics, experimental and structure refinement details for crystal structure of complexes (**2**) and (**3**).

	Complex (**2**)	Complex (**3**)
Empirical formula	$C_{15}H_{33}AuNPS_2$	$C_{17}H_{37}AuNPS_2$
Empirical formula weight	519.48	547.53
Crystal size/mm	0.2 × 0.2 × 0.05	0.1 × 0.1 × 0.1
Wavelength/Å	0.71073	0.71073
Temperature/K	200	200
Crystal symmetry	Monoclinic	Orthorhombic
Space group	P 21/c	P 21 21 21
a/Å	14.3661 (9)	13.6063 (8)
b/Å	12.5419 (6)	13.6398 (9)
c/Å	11.6216 (7)	23.7965 (13)
β/°	103.910 (6)	90
V/Å^3	2032.6 (2)	4416.3 (5)
Z	4	8
Dc/Mg m^{-3}	1.698	1.647
μ(Mo-Kα)/mm^{-1}	7.515	6.922
F(000)	1024	2176
θ Limits/°	3.1–29.0	3.0–29.1
Collected reflections	10518	37465
Unique reflections(R_{int})	4774 (0.043)	9929 (0.043)
Observed reflections [$F_o > 2\sigma(F_o)$]	3391	10949
Goodness of fit on F2	1.03	1.05
$R_1(F)$,^{a}[$I > 2\sigma(I)$]	0.037	0.035
wR_2 (F2),^{b}[$I > 2\sigma(I)$]	0.095	0.082
Largest diff. peak, hole/e Å^{-3}	0.93, −1.78	3.26, −0.73
Flack (Absolute structure parameter)	–	−0.008 (6)

Table 6
Selected bond angles (Å) and bond lengths (°) for complexes (**2**) and (**3**).

Bond lengths (Å)		Bond angles (°)	
Complex (**2**)			
Au1–P1	2.2743 (14)	P1–Au1–S1	176.44 (4)
Au1–S1	2.3247 (15)	C1–S1–Au1	99.66 (17)
Complex (**3**)			
Au1–P1	2.2818 (15)	P1–Au1–S1	172.74 (6)
Au1–S1	2.3293 (15)	C1–S1–Au1	101.7 (2)
Au2–P2	2.2753 (16)		
Au2–S3	2.3139 (16)		

Acknowledgment

The author(s) would like to acknowledge the support provided by King Abdulaziz City for Science and Technology (KACST) through the Science & Technology Unit at King Fahd University of Petroleum & Minerals (KFUPM) for funding this work through project No. ***14-MED64-04*** as part of the National Science, Technology and Innovation Plan.

Appendix A. Supplementary data

Supplementary data related to this article can be found at http://dx.doi.org/10.1016/j.ejmech.2015.03.019.

References

[1] B. Rosenberg, L. Van Camp, T. Krigas, Nature 205 (1965) 698–699.
[2] Y. Kidani, M. Noji, T. Tashiro, Gann 71 (1980) 637–643.
[3] N.J. Wheate, S. Walker, G.E. Craig, R. Oun, Dalton Trans. 39 (2010) 8113–8127.
[4] E. Wong, C.M. Giandomenico, Chem. Rev. 99 (1999) 2451–2466.
[5] V.G. Schweitzer, Otolaryngol. Clin. North Am. 26 (1993) 759–789.
[6] D.J. Stewart, Crit. Rev. Oncol. Hematol. 63 (2007) 12–31.
[7] S. Dhar, S.J. Lippard, Current status and mechanism of action of platinum-based anticancer drugs, in: E. Alessio (Ed.), Bioinorganic Medicinal Chemistry, Wiley-VCH Verlag GmbH & Co. KGaA, Weinheim, Germany, 2011, pp. 79–93.
[8] K. Nomiya, R.S. Yamamoto, R. Noghuchi, H. Yokoyama, N.C. Kasuga, K. Ohyama, C. Kato, J. Inorg. Biochem. 95 (2003) 208–220.
[9] T. McCormick, W.L. Jia, S. Wang, Inorg. Chem. 45 (2006) 147–155.
[10] S.S. Al-Jaroudi, M.I.M. Wazeer, A.A. Isab, S. Altuwaijri, Polyhedron 50 (2013) 434–442.
[11] R.B. Bostancioglu, K. Isik, H. Genc, K. Benkli, A.T. Koparal, J. Med. Chem. 27 (2012) 458–466.
[12] S.H. van Rijt, P.J. Sadler, Drug Discov. Today 14 (2009) 1089–1097.
[13] R. Noghuchi, A. Hara, A. Sugie, K. Nomiya, Inorg. Chem. Commun. 9 (2006) 355–359.
[14] K. Nomiya, R. Noghuchi, K. Ohsawa, K. Tsuda, M. Oda, J. Inorg. Biochem. 78 (2000) 363–370.
[15] B.P. Howe, Met-Based Drugs 4 (1997) 273–277.
[16] C. Frank Shaw III, Chem. Rev. 99 (1999) 2589–2600.
[17] O. Crespo, V.V. Brusko, M.C. Gimeno, M.L. Tornil, A. Laguna, N.G. Zabirov, Eur. J. Inorg. Chem. 2 (2004) 423–430.
[18] K. Nomiya, R. Noghuchi, M. Oda, Inorg. Chim. Acta 298 (2000) 24–32.
[19] H.Q. Liu, T.-C. Cheung, S.-M. Peng, C.-M. Che, J. Chem. Soc. Chem. Commun.

(1995) 1787–1788.
[20] C.J. O'Connor, E. Sinn, Inorg. Chem. 17 (1978) 2067–2071.
[21] M.A. Cinellu, G. Minghetti, M.V. Pinna, S. Stoccoro, A. Zucca, M. Manassero, M. Sansoni, J. Chem. Soc. Dalton Trans. (1998) 1735–1742.
[22] K. Nomiya, S. Takahashi, R. Noghuchi, J. Chem. Soc. Dalton Trans. (2000) 2091–2097.
[23] R.C. Elder, K. Ludwig, J.N. Cooper, M.K. Eidsness, J. Am. Chem. Soc. 107 (1985) 5024–5025.
[24] R.W.-Y. Sun, C.-M. Che, Coord. Chem. Rev. 253 (2009) 1682–1691.
[25] P. Papathanasiou, G. Salem, P. Waring, A.C. Willis, J. Chem. Soc. Dalton Trans. (1997) 3435–3443.
[26] H. Lv, B. Yang, J. Jing, Y. Yu, J. Zhang, J.-L. Zhang, Dalton Trans. 41 (2012) 3116–3118.
[27] T.M. Simon, D.H. Kunishima, G.J. Vibert, A. Lorber, Cancer 44 (1979) 1965–1975.
[28] M.J. McKeage, P. Papathanasiou, G. Salem, A. Sjaarda, G.F. Swiegers, P. Waring, S.B. Wild, Metal-Based Drugs 5 (1998) 217–223.
[29] S.J. Berners-Price, C.K. Mirabelli, R.K. Johnson, M.R. Mattern, F.L. Mccabe, L.F. Faucette, C.M. Sung, S.M. Mong, P.J. Sadler, S.T. Crooke, Cancer Res. 46 (1986) 5486–5493.
[30] V. Gandina, A.P. Fernandes, M.P. Rigobello, B. Dani, F. Sorrentino, F. Tisato, M. Björnstedt, A. Bindoli, A. Sturaro, R. Rella, C. Marzano, Biochem. Pharm. 79 (2010) 90–101.
[31] I. Ott, X. Qian, Y. Xu, D.H.W. Vlecken, I.J. Marques, D. Kubutat, J. Will, W.S. Sheldrick, P. Jesse, A. Prokop, C.P. Bagowski, J. Med. Chem. 52 (2009) 763–770.
[32] S. Tian, F.-M. Siu, S.C.F. Kui, C.-N. Lok, C.-M. Che, Chem. Commun. 47 (2011) 9318–9320.
[33] L. Ronconi, L. Giovagnini, C. Marzano, F. Bettio, R. Graziani, G. Pilloni, D. Fregona, Inorg. Chem. 44 (2005) 1867–1881.
[34] V. Milacic, D. Chen, L. Ronconi, K.R. Landis-Piwowar, D. Fregona, Q.P. Dou, Cancer Res. 66 (2006) 10478–10486.
[35] X. Zhang, M. Frezza, V. Milacic, L. Ronconi, Y. Fan, C. Bi, D. Fregona, Q.P. Dou, J. Cell. Biochem. 109 (2010) 162–172.
[36] E.R. Tiekink, Crit. Rev. Oncol. Hematol. 42 (2002) 225–248.
[37] F.K. Keter, I.A. Guzei, M. Nell, W.E. van Zyl, J. Darkwa, Inorg. Chem. 53 (2014) 2058–2067.
[38] A.J. Odola, J.A.O. Woods, J. Chem. Pharm. Res. 3 (2011) 865–871.
[39] F. Jian, Z. Wang, Z. Bai, X. You, H. Fun, K. Chinnakali, L.A. Razak, Polyhedron 18 (1999) 3401–3406.
[40] A. Jayaraju, M.M. Ahamad, R.M. Rao, J. Sreeramulu, Der. Pharma. Chem. 4 (2012) 1191–1194.
[41] H. Nabipour, S. Ghammamy, S. Ashuri, Z.S. Aghbolagh, J. Org. Chem. 2 (2010) 75–80.
[42] J. Chatt, L.A. Duncanson, L.M. Venanzi, Nature 177 (1956) 1042–1043.
[43] I. Raya, I. Baba, B.M. Yamin, Malays. J. Anal. Sci. 10 (2006) 93–98.
[44] W. Haas, T. Schwarz, Microchem. Ichonal. Acta 58 (1963) 253–259.
[45] D.C. Onwudiwe, P.A. Ajibade, Polyhedron 29 (2010) 1431–1436.
[46] C.J. Pouchert, Aldrich Library of FT-IR Spectra, second ed., Aldrich Chemical Company, Milwaukee, 1997.
[47] D.L. Pavia, G.M. Lampman, S.G. Kriz, Introduction to Spectrochemistry, third ed., Thomson Learning, USA, 2001.
[48] R.M. Silverstein, F.X. Webster, Spectrometric Identification of Organic Compounds, sixth ed., Wiley, New York, 1998.
[49] T.W.G. Solomons, C. Fryhle, Study Guide to Organic Chemistry. Organic Chemistry, seventh ed., Wiley, New York, 2000.
[50] K.N. Kouroulis, S.K. Hadjikakou, N. Kourkoumelis, M. Kubicki, L. Male, M. Hursthouse, S. Skoulika, A.K. Metsios, V.Y. Tyurin, A.V. Dolganov, E.R. Milaevag, N. Hadjiliadis, Dalton Trans. (2009) 10446–10456.
[51] E.A. Allen, W. Wilkinson, Spectrochim. Acta 28 (1972) 2257–2262.
[52] I.S. Butler, A. Neppel, K.R. Plowman, C.F. Shaw, J. Raman Spectrosc. 15 (1984) 310–318.
[53] A.G. Jones, D.B. Powell, Spectrochim. Acta 40 (1984) 563–570.
[54] S.Y. Ho, E.R.T. Tiekink, Z. Krist. 220 (2005) 342–344.
[55] I. Sänger, H.-W. Lerner, T. Sinke, M. Bolte, Acta Cryst. E68 (2012) m708.
[56] P. Lu, T.C. Boorman, A.M.Z. Slawin, I. Larrosa, J. Am. Chem. Soc. 132 (2010) 5580–5581.
[57] R.E. Marsh, Acta Cryst. B58 (2002) 893–899.
[58] M. Altaf, M. Monim-ul-Mehboob, A.A. Isab, V. Dhuna, G. Bhatia, K. Dhuna, S. Altuwaijri, New. J. Chem. 39 (2015) 377–385.
[59] M. Serratrice, M.A. Cinellu, L. Maiore, M. Pilo, A. Zucca, C. Gabbiani, A. Guerri, I. Landini, S. Nobili, E. Mini, L. Messori, Inorg. Chem. 51 (2012) 3161–3171.
[60] I. Ott, R. Gust, Arch. Pharm. Chem. Life Sci. 340 (2007) 117–126.
[61] E. Barreiro, J.S. Casas, M.D. Couce, A. Sánchez, A. Sánchez-Gonzalez, J. Sordo, E.M. Vázquez-López, J. Inorg. Biochem. 138 (2014) 89–98.
[62] E. Barreiro, J.S. Casas, M.D. Couce, A. Sánchez, J. Sordo, E.M. Vázquez-López, J. Inorg. Biochem. 131 (2014) 68–75.
[63] R. Kivekäs, E. Colacio, J. Ruiz, J.D. López-González, P. León, Inorg. Chim. Acta 159 (1989) 103–110.
[64] L. Ortego, F. Cardoso, S. Martins, M.F. Fillat, A. Laguna, M. Meireles, M.D. Villacampa, M.C. Gimeno, J. Inorg. Biochem. 130 (2014) 32–37.
[65] I. Ott, T. Koch, H. Shorafa, Z. Bai, D. Poeckel, D. Steinhilber, R. Gust, Org. Biomol. Chem. 3 (2005) 2282–2286.
[66] Agilent, Crys Alis PRO, Agilent Technologies Yarnton, England, 2011.
[67] G.M. Sheldrick, Acta Cryst. A64 (2008) 112–122.
[68] (1.0.4, gui:1.0.3) (C), SCALE3 ABSPACK an Oxford Diffraction Program, Oxford Diffraction Ltd, 2005.
[69] C.F. Macrae, P.R. Edgington, P. McCabe, E. Pidcock, G.P. Shields, R. Taylor, M. Towler, J. van de Streek, J. Appl. Cryst. 39 (2006) 453–457.
[70] M.B. Hansen, S.E. Nielsen, K. Berg, J. Immunol. Methods 119 (1989) 203–210.